Development of Printability of Bio-Composite Materials Using *Luffa cylindrica* Fiber

Sinan Sonmez

This study examined the surface adhesion of ink on bio-composite materials that were produced using *Luffa cylindrica* fiber and epoxy. To increase the ink adhesion on the surface, two different production methods were developed. The surface roughness and the surface contact angle of the bio-composite surfaces manufactured by each method were determined. The printing was applied on the surface of the bio-composite materials using a screen-printing procedure. While keeping the printing conditions constant, two different ink types, environmentally friendly water-based ink and solvent-based ink, were utilized. As a result of this study, the two types of ink were adhered on the polymer-coated surface, and there was no adhesion on the uncoated surfaces. In addition, the printability of the solvent-based ink was better than the water-based one, and the image of the transfer had higher quality. When the water or solvent-based inks were applied on the surface, the groups capable of forming hydrogen bonds, which were present in both kinds of ink, constituted hydrogen bonds with the C=O and N-H groups. This resulted in better adhesion on the surface, which was due to the presence of the separator.

Keywords: Luffa cylindrica fiber; Bio-composite; Printability; Polymer coating; Ink

Contact information: Department of Printing Technologies, School of Applied Sciences, Marmara University, Goztepe Campus, Kadikoy, Istanbul, 34720 Turkey; E-mail: ssonmez@marmara.edu.tr

INTRODUCTION

Increasing environmental awareness has motivated researchers to design environmentally friendly materials (Mohanta and Acharya 2013). Plant fibers have received greater attention due to their abundance, suitability as a renewable resource, biodegradability, and cost effectiveness (Tanobe *et al.* 2014; Koruk and Genc 2015). The popularity of natural fiber reinforced composites has increased in the 21st century. The use of natural fiber reinforced polymeric composites is popular in many applications due to their ready availability, low cost, low weight, high specific modulus, non-toxicity, and cleanliness (Mohanta and Acharya 2015). As cellulosic fiber is natural and biodegradable, the degradation products are not harmful to the environment. Additionally, during production, there is less carbon dioxide released into the atmosphere. The lightness of the material is beneficial also, allowing a wide range of potential uses for natural fiber reinforced composites (Bismarck *et al.* 2006).

The performance of the fiber reinforced composite materials under prolonged immersion in water and exposure to wind, rain, or sun is better than for other conventional construction materials (Scudamore and Cantwell 2002). Thus, numerous environmental organizations declared that the majority of products used in automotive and paper industries, as well as railways and roads, need to use recyclable material. As a result, the

amount of fiber used in the production of composites has increased to about 45% in Europe and the USA (Mohanty *et al.* 2000).

All of the required information related to the product inside the package needs to be present on the composite surface of the package. Screen printing, a simple and efficient method, is a printing technique mainly suited for flat or moderately flat surfaces, and has the advantages of simplicity, low cost, controllable thickness, and uniformity of film. There are the advantages of possible recycling and cleaning for inks used in this printing system (Wang *et al.* 2009).

This study concentrated on *Luffa cylindrica* fiber, which is a tropical plant widely available in the wet and warm climates of the world, and it is especially abundant along the Mediterranean coast of Turkey (Koçak 2008; Genc and Koruk 2016a). In this study, *Luffa cylindrica* fiber harvested from the Mediterranean coast of Turkey was molded using an epoxy resin, and a bio-composite structure was obtained. Environmentally friendly water-based ink and solvent-based ink, which are used widely in the industry, were each printed on the bio-composite material surface using the screen-printing technique. After the printing, the ink adhesion on the surface of the bio-composite materials, their roughness, and light-fastness were investigated. The morphological properties of the bio-composite were determined by scanning electron microscopy (SEM). The behavior of bio-composite structures was analyzed *via* Fourier transform infrared spectroscopy (FT-IR) to determine the ink adhesion interface on the bio-composite surface.

EXPERIMENTAL

Materials

Luffa cylindrica fiber was used as reinforcement, and the epoxy resin was utilized as a matrix to manufacture the bio-composite laminate specimens. The properties of the liquid epoxy resin are given in detail in Table 1. Luffa fibers were prepared without any surface treatment to observe the potential use as a core material in hybrid composites, as previously described (Genc 2015). Bio-composites were produced under two different conditions. Bio-composite plates were produced with and without a polyester separator between the bio-composite part and the mold. The bio-composite samples produced without a separator were labeled as Basic bio-composite (BC), and the ones with a separator were named Separator effected bio-composite (SEC).

Table 1. Properties of the Liquid Epoxy Resin (Duratek 2016)

Test	Method	Value
Liquid resin properties		
Color	Observation	Transparent
Density	DIN EN ISO 2811-1 (2016)	1.15 kg/L
Viscosity	ASTM D1545-07 (2012)	330 mPa.s
Pot life	DIN 16945 (1989)	170’
Test	Method	Pure resin value
Rigid resin mechanical properties		
Flexural strength	DIN EN ISO 178 (2013)	125 N/mm^2
Elasticity modulus	DIN EN ISO 527-2 (2012)	3200 N/mm^2
Elongation at break	DIN EN ISO 527-2 (2012)	3.75%
Tensile strength	DIN EN ISO 527-2 (2012)	75 N/mm^2
Water absorption	DIN EN ISO 175 (2011)	46.5 mg

The effect of the separator on the bio-composite surface was examined to understand the ink adhesion on the surface. As shown in Fig. 1a, the specimens were compressed on the Y-axis using a hot hydraulic press machine to shape the bio-composites and cure the epoxy resin at the same time. The lower plate was fixed to the machine frame, while the upper plate was controlled by a programmable logic controller (PLC) system with 5 bars of pressure to compress the stacked laminates. The heat was adjusted to 80 °C during the curing process, which lasted about 300 min (Genc and Koruk 2016b). The bio-composite was then taken out of the mold. When a separator was used in the second method, the polyester sheet was removed from the bio-composite surface. The coated and uncoated bio-composite plates are shown in Fig. 1b and 1c, respectively.

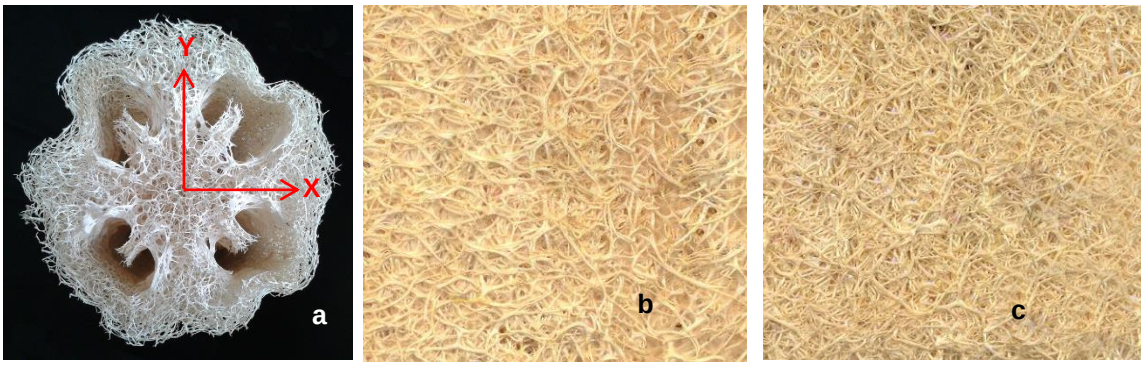

Fig. 1. a) *Luffa cylindrica* fiber, b) BC, and c) SEC (magnification at 60%)

Methods

The chemical structures of the synthesized monomer were identified by FT-IR. The FT-IR spectrum was recorded on a Shimadzu 8303 FT-IR spectrometer (Shimadzu Corporation, Kyoto, Japan). The surface roughness of these bio-composite materials was measured using a portable MarSurf M 300 roughness measurement device (Mahr GmbH, Göttingen, Germany) with a 5.6 mm traversing length according to DIN EN ISO 4288 (1998), and the values of the surface roughness "a" (R_a; arithmetic average of absolute values) and the surface roughness "z" (R_z; average distance between the highest peak and lowest valley in each sampling length) were recorded.

The contact angle of the BC and SEC samples was measured using a PG-X Goniometer (Paul N. Gardner Company, Inc., FL, USA) based on TAPPI T 558 (2010). One color printing with environmentally friendly water-based black ink or solvent-based black ink was applied on the BC and SEC samples through the screen-printing technique. The equipment used for printing was a semi-automatic screen-printing machine. The mesh number was 120 threads per cm (tpc), and the dot per cm was 40 (dpc). The angle of the squeegee was 45°, and the hardness of squeegee was 75 Shore (Akgul *et al.* 2013). The density values of the BC and SEC samples were measured by a Gretag Macbeth SpectroEye instrument (45/0°) (X-Rite, Inc., MI, USA). Also, the CIE *L**, *a**, and *b** values of the BC and SEC samples were measured by the D50 illuminant/2° observer values using the same instrument.

The gloss values of the BC and SEC samples were determined using a BYK Portable glossmeter (BYK-Gardner Gmbh, Geretsried, Germany) based on ISO 2813 (2014). Finally, the delta gloss of the BC and SEC samples were evaluated. The morphology and phase compositions of the BC and SEC samples were determined by SEM (JSM-5910 LV, JEOL Ltd., Tokyo, Japan) after Au-Pd coating (Ilhan 2014). The IPC-TM-

650 Adhesion, Tape Testing Method was performed to test the ink adhesion on the bio-composite surface (IPC 2016).

RESULTS AND DISCUSSION

Surface Properties

The surface roughness and smoothness are important parameters to obtain a qualified print image. A smoother surface and sharper image results in a more resolved print image (Elmas and Sonmez 2011). R_a values closer to zero indicate a smoother surface. The R_a values, which were obtained using a MarSurf M 300 roughness measurement device, are given in Table 2.

Table 2. BC *vs.* SEC Sample Roughness Values

Roughness	R_a (µm)
BC	0.9
SEC	1.6

Bio-composites with a low surface energy have high contact angles, which indicate poor ink wettability (Sonmez 2011). Figure 2 illustrates the angle curves for the 20 s dynamic contact angle experiments. A steeply declining curve reflects fast ink spreading on the BC and SEC surface.

During the 20 s test, the contact angles of the samples declined slowly, indicating that there was less ink spreading or ink immobilization. This could provide improved image resolution and sharpness. The contact angle assessed on the BC surface was higher than on the SEC surface, which showed that the SEC surface was hydrophilic. This was an important factor for ink adhesion during the printing process. Figures 3 and 4 show the very first moment of the drop and its spread after 20 s on the BC and the SEC samples, respectively.

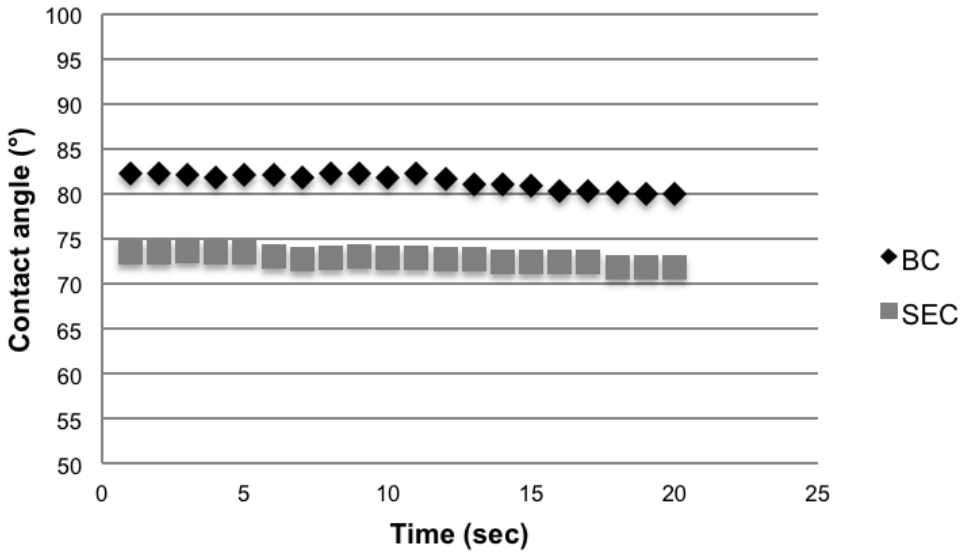

Fig. 2. Contact angle values of the BC and SEC samples

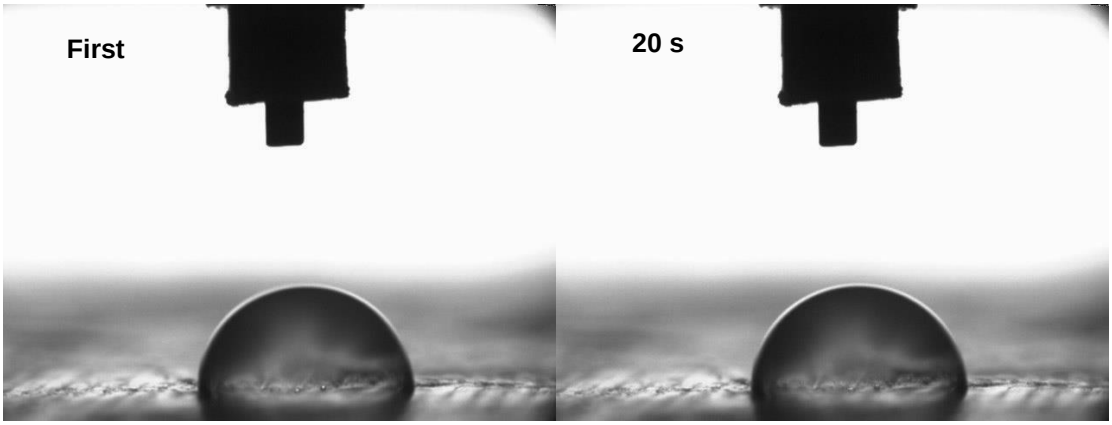

Fig. 3. Drop views on the BC samples in the first and 20th s

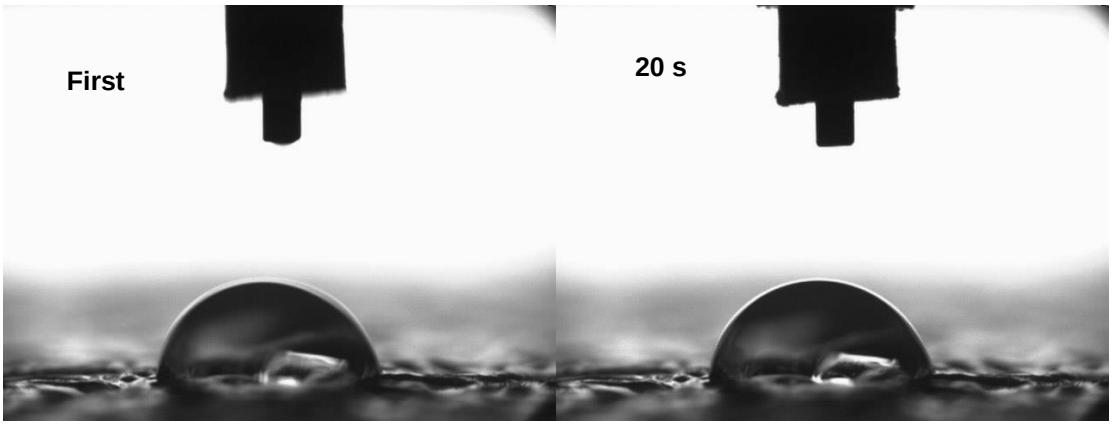

Fig. 4. Drop views on the SEC samples in the first and 20th s

Printability Properties

Print density

The print density is an important factor for a good quality print due to its determinant effect on the contrast between the print and substrates (Zang and Aspler 1995). The physical properties of the paper, such as smoothness and porosity, are prime factors for optimal print density. In addition, paper permeability has as much of an effect on print density as porosity.

The print density is affected by the kind of coating pigment and ink ingredients used. Mechanical and environmental print conditions are also deterministic factors for optimal print density (Biricik *et al.* 2011).

The printing density values of the BC and SEC samples were compared. For printing with the water-based ink, the utilization of SEC did not affect the density value, while the use of SEC increased the density values slightly for the printing performed with the solvent-based ink. For both of the BC and SEC samples, the density values obtained using the solvent-based ink were better than those resulting from the water-based ink (Fig. 5).

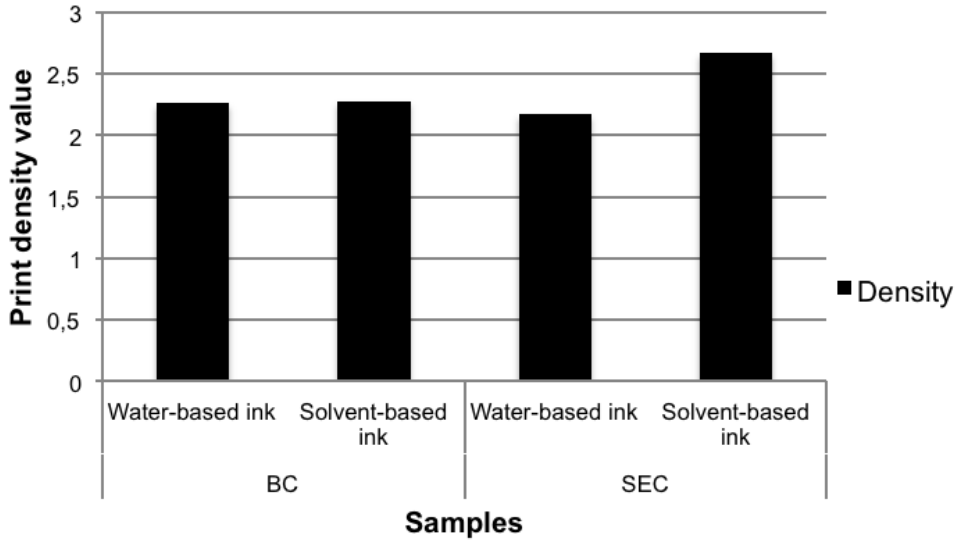

Fig. 5. Print density of the BC and SEC samples

Print lightness

The *L** values of the printing made using the water and solvent-based inks on the bio-composite materials are given in Fig. 6. The lightness value, which ranges from 0 to 100, shows the saturation of the color. Darker print is nearer to 0, and lighter print is nearer to 100 (Viscarra Rossela *et al.* 2006).

The printing lightness value obtained from the solvent-based ink was lower than the one acquired from the water-based ink. Thus, the color saturation attained by the printing using the water-based ink was lower than for the printing with the solvent-based ink. In other words, the obtained shade for the water-based ink printing was lighter than what was desired. The utilization of the separator did not alter the *L** value of the printing with the solvent-based ink, while the *L** value of the printing with the water-based ink increased noticeably.

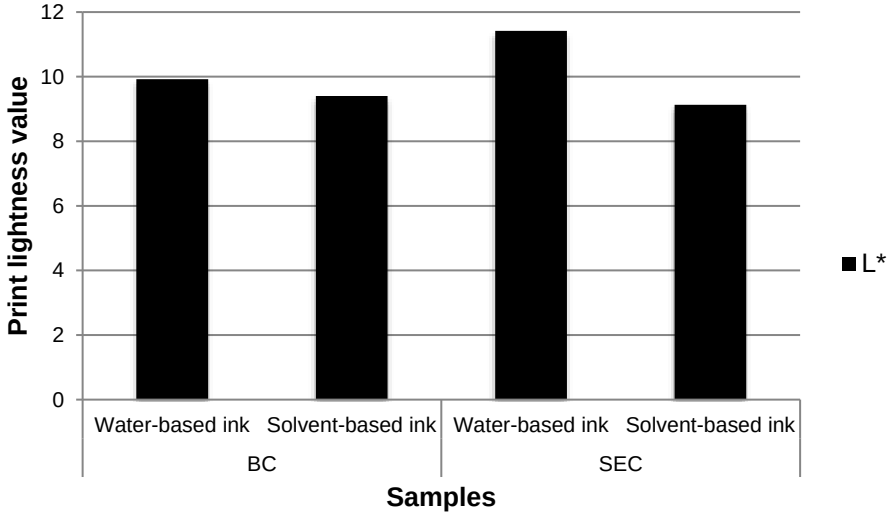

Fig. 6. Print lightness of the BC and SEC samples

Delta gloss

The delta gloss, which is the difference between the gloss before and after printing (at the same angle) (Johnson *et al*. 2009), is an indicator of a good glossy print. The final gloss values may increase or decrease depending on the surface roughness and the porosity properties of the paper and ink ingredients (Juuti *et al.* 2007). In particular, the binder of the ink ingredients and its amount are useful predictors of the glossy print quality (Béland *et al.* 2000).

Table 3. Delta Gloss of BC Samples

Inks	Gloss Before Printing	Gloss After Printing	Delta Gloss
Water-based ink	4	18	14
Solvent-based ink	4	20	16

Both the water and solvent-based ink printings on the BC samples increased the gloss values, as shown in Table 3. The increase in the gloss value after printing indicated brighter printings.

The gloss value of the SEC samples before printing was higher than the BC samples, as presented in Table 4. This showed that the separator augmented the brightness of the bio-composite material. However, the delta gloss values of the SEC samples decreased after printing, which indicated that the printing brightness of the BC samples was higher than the SEC samples. This was an important feature amongst the printability parameters, as the visual quality was advanced.

Table 4. Delta Gloss of SEC Samples

Inks	Gloss Before Printing	Gloss After Printing	Delta Gloss
Water-based ink	11	8	-3
Solvent-based ink	11	9	-2

Print chroma

The chroma refers to the color, and it can be measured through the color intensity or saturation (Preston *et al.* 2002). A high chroma indicates high color saturation, which is an important property for good quality prints. Another important property is high color gamut. The print chroma value (C_{ab}) was calculated by Eq. 1 (Fairchild 2004).

$$C_{ab} = \sqrt{a^{*2} + b^{*2}} \quad (1)$$

For a^*, negative values indicate green, while positive values indicating magenta. For b^*, negative values indicate blue, and positive values indicate yellow.

The print chroma values of the BC and SEC samples are shown in Fig. 7. The print chroma value of the printing using the water-based ink was lower than for the solvent-based ink, which showed that there is the possibility of attaining of a wider color range on the SEC surfaces. This was an important parameter for defining the printing quality.

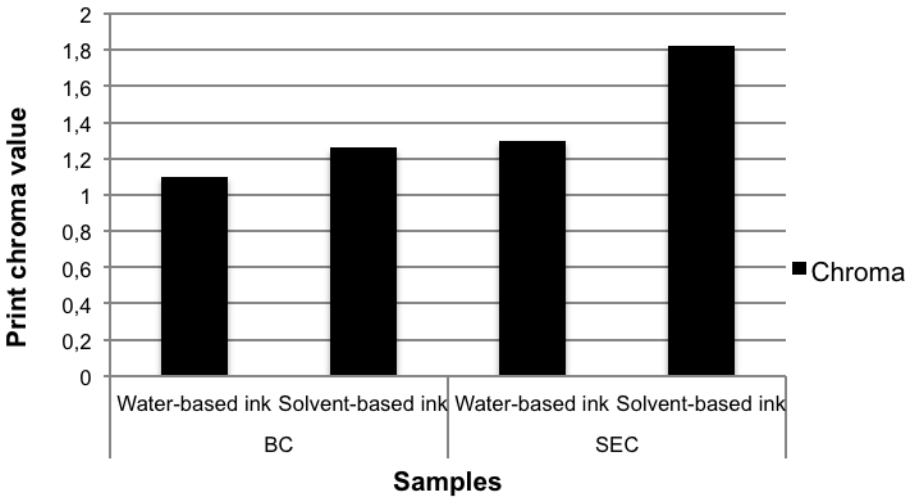

Fig. 7. Print chroma of the BC and SEC samples

Ink adhesion

According to the method mentioned in the Experimental section, the insulating tape was stuck on the bottom printing side for both the water and solvent-based ink printings, and the insulating tape was later removed from the surface. After this procedure, the ink was removed with the insulating tape from the BC surfaces, while the ink remained on the SEC surfaces for both types of ink. The testing procedure of the printing with the solvent-based ink is shown in Figs. 8 and 9.

The results after testing revealed that the ink was adhered only physically *via* drying on the BC surface. Thus, the ink was removed from the surface, which indicated that the permanent adhesion of the ink on the BC surface, the most important characteristic of printability, did not occur.

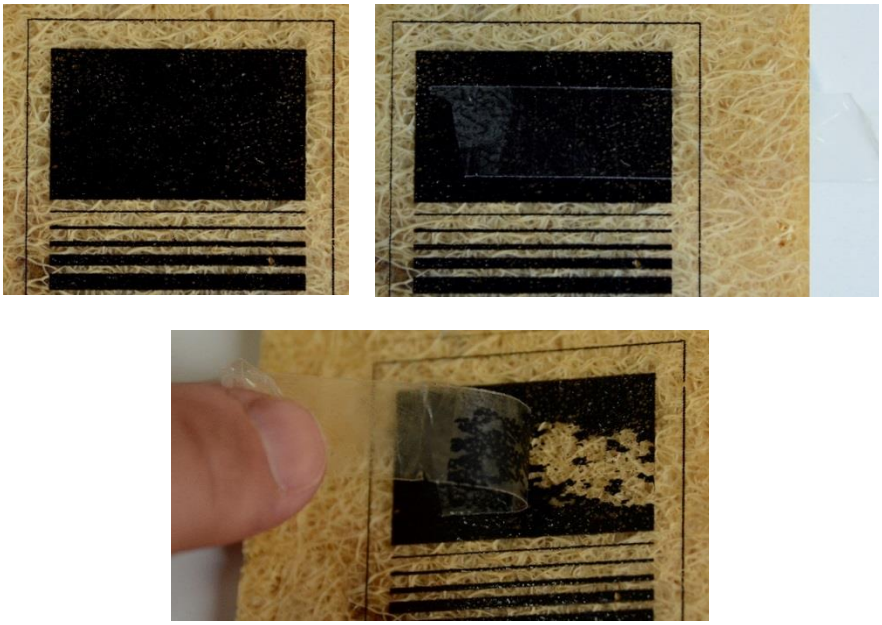

Fig. 8. The hold out of the ink on the BC surface

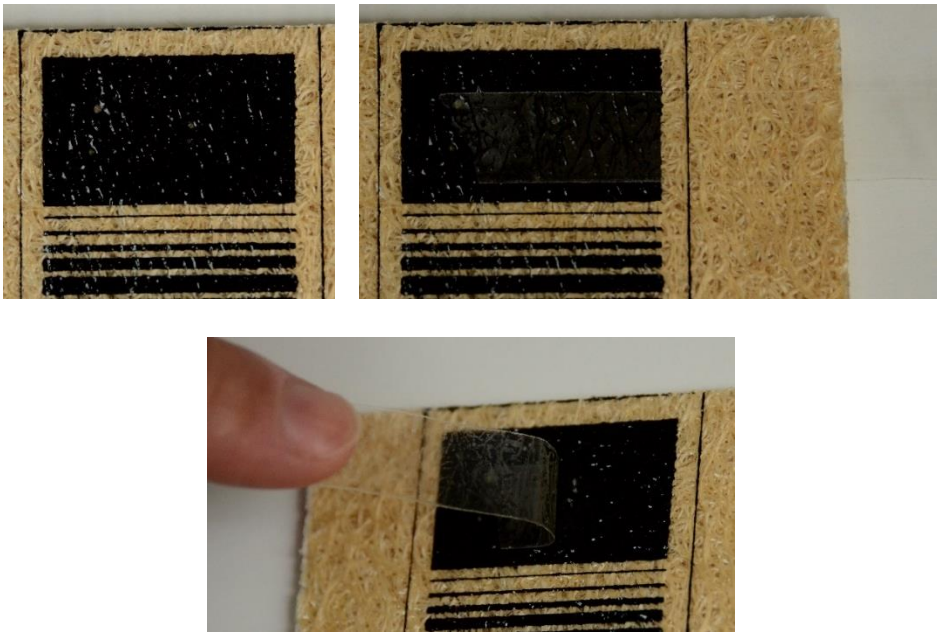

Fig. 9. The hold out of the ink on the SEC surface

FT-IR spectrum

In Fig. 10a, the absorbance peaks in the range of 300 to 3500 cm^{-1} belonged to the H_2O molecules' –OH stretching peaks absorbed on the BC material. The peaks located between 2850 and 3100 cm^{-1} were the stretching peaks of the C-H groups within the epoxy resin. The adsorption peak of the C-H groups on the distortion (flexion) mode was seen at 1450 cm^{-1}. In this spectrum, the C-O-C stretching peak of the epoxy ring was clearly present at 1200 cm^{-1}. The peak in the range of 1000 to 1100 cm^{-1} indicated that ether (C-O-C) groups formed after the cure (cross-linking) of the epoxy resin.

The FT-IR spectrum of the polymer separator is shown in Fig. 10b. This spectrum revealed that the separator film was a poly-amid (a mixture of NYLON 6-NYLON 6,6) (Khalid and Mohammad 2009). The sharp peaks at 3300 cm^{-1} and 3200 cm^{-1} were the stretching absorbance peaks of two different N-H groups. The distortion peaks of the N-H groups were clearly evident at 1520 cm^{-1}. The peaks situated in the range of 2900 to 3000 cm^{-1} were the stretching peaks of the C-H groups. The absorbance peak of the carbonyl groups in the poly-amide structure (C=O) groups was found at about 1630 cm^{-1}.

Figure 10c shows the FT-IR spectrum taken from the surface of the composite material prepared using the poly-amid based separator film. This spectrum was similar to the FT-IR spectrum of the separator film in Fig. 10b. Hence, the poly-amid based separator film was fully adhered/absorbed on the epoxy based bio-composite surface during production. As this bonding occurred at an elevated temperature, covalent bonding was expected to form. The stable adhesion of the poly-amid film *via* covalent bonding caused the bio-composite surface functionalization with the C=O and N-H groups, which could cause hydrogen bonding at the same time. In other words, the surface of the epoxy based bio-composite material was modified to adhere the ink more stably on the surface by forming hydrogen bonds. When the water or solvent-based inks were applied on the surface, the groups capable of forming hydrogen bonds, which were present in both kinds of ink, constituted hydrogen bonds with the C=O and N-H groups and resulted in the better and more qualified adhesion of ink on the surface.

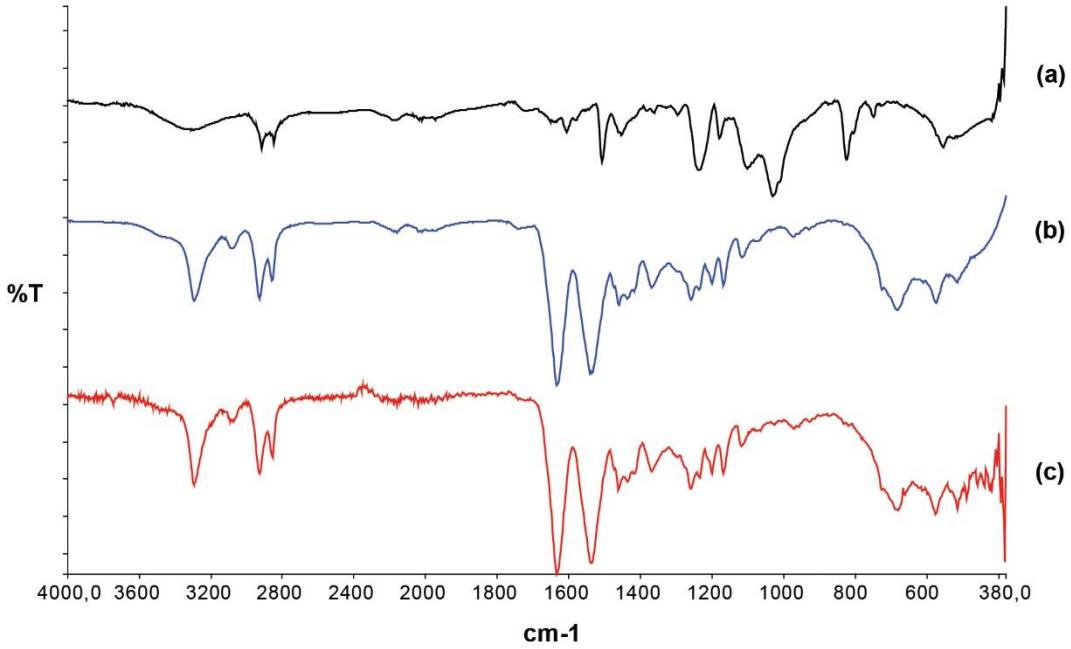

Fig. 10. FT-IR spectra of (a) the bio-composite surface prepared without the separator (BC), b) the polymer separator, and c) the bio-composite surface prepared with the separator (SEC). The FT-IR spectra were taken using the Attenuated Total Reflectance (ATR) module. The spectra represent the functional groups on the material surface.

Figure 11 shows the FT-IR spectra of the surfaces with the separator film (Fig. 11a) and after application of the water-based (Fig. 11b) and solvent-based inks (Fig. 11c). The loss of the characteristic peaks of the poly-amid structure on the ink-transferred surfaces revealed that the ink perfectly bonded/adhered on the surface and completely covered the surface by wetting in a compatible manner.

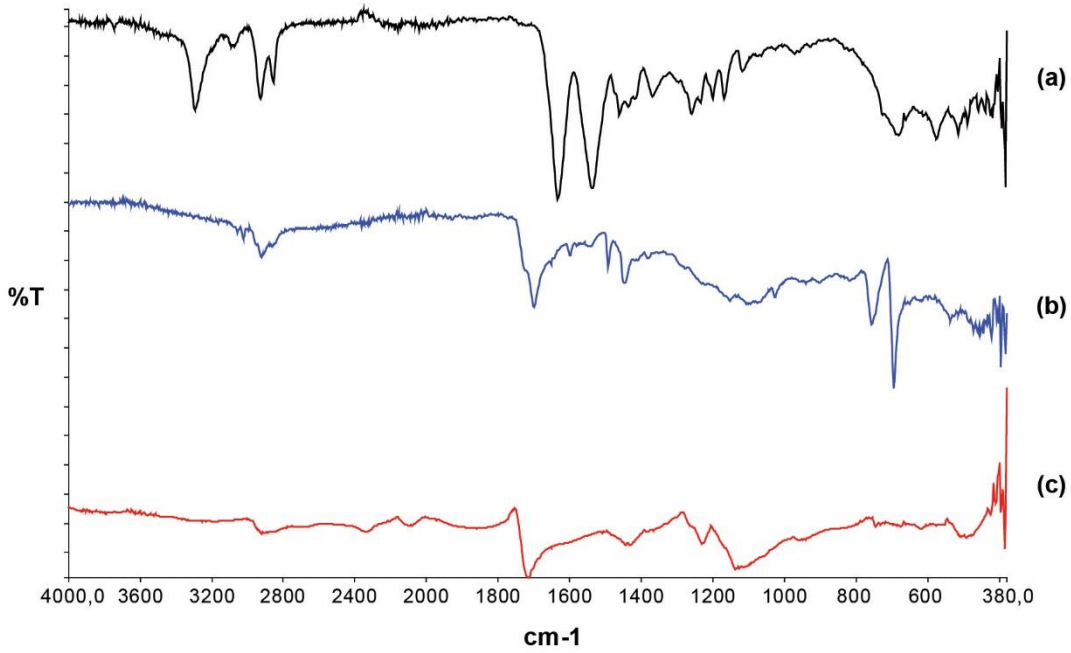

Fig. 11. FT-IR spectra of a) the SEC surface, b) the water-based ink applied on the SEC surface, and c) the solvent-based ink applied on the SEC surface

SEM micrographs

The SEM-BE (backscattered electron) micrographs of both the BC and SEC samples are given in Fig. 12. The micrographs showed the ink layer and mold structures. There was no chemical bonding between the substrate and the ink. Rather, there was an interaction between the functional groups of the polymer molecules with the substrate surface, which could not be visualized by the SEM system.

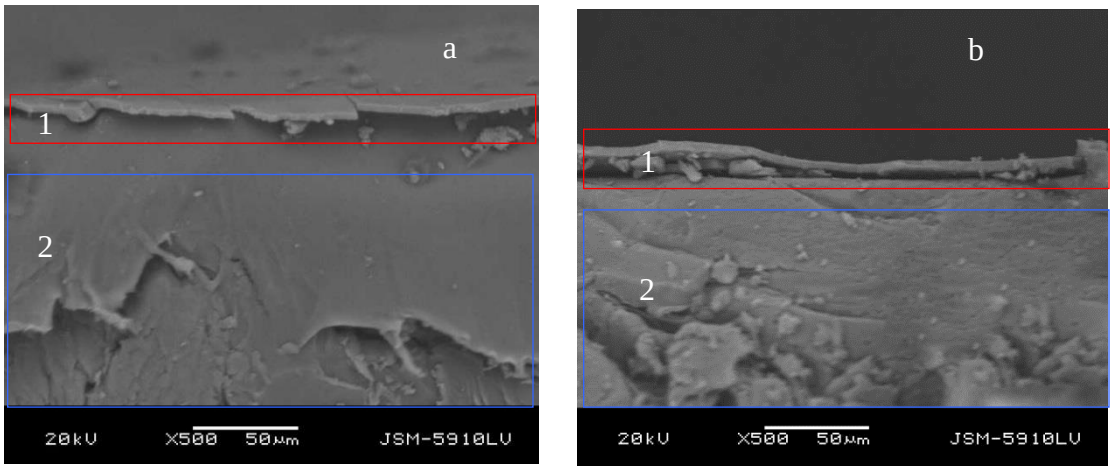

Fig. 12. SEM-BE micrographs at 500 times magnification. (a) BC sample; (b) SEC sample. (1) indicates the ink layer, and (2) indicates the mold structures.

CONCLUSIONS

1. It was discovered after the production of the bio-composite materials without the use of the separator that there was no adequate adhesion of the ink due to physical drying on the surface.
2. Without the use of the separator on the surface, only the cross-linking of the epoxy resin occurred. It was determined by the FT-IR spectra that the poly-amid based separator film was fully adhered/absorbed on the epoxy based bio-composite material's surface during the production process. In other words, the surface of the epoxy based bio-composite material was modified in order to adhere the ink more stably on the surface by forming hydrogen bonds. When the environmentally friendly water-based ink or solvent-based ink were applied on the surface, the groups capable of forming hydrogen bonds, which were present in both kinds of ink, constituted hydrogen bonds with the C=O and N-H groups. This resulted in better and more qualified adhesion of ink on the surface, which was due to the presence of the separator.
3. For both of the surfaces, the obtained printing density, delta gloss, and chroma values were all higher for the solvent-based ink, which indicated that the visual quality was better for the solvent-based ink printing on the bio-composite material made by *Luffa cylindrica* fiber. Also, as the surface of the bio-composite materials was very hydrophobic, the solvent-based ink in the printing process displayed better performance and printability compared to the environmentally friendly water-based ink during the image transfer on the bio-composite material and drying stages.

4. The use of the separator improved the gloss values noticeably, while it resulted in no large difference in the values of print density, chroma, and lightness values.

REFERENCES CITED

Akgül, A., Şahinbaşkan, T., and Yilmaz, S. B. (2013). "Effects of enzymatic pre-treatments on printing of cotton knitted fabrics," in: *Proceedings of 2nd International Conference on Value Addition and Innovation in Textiles*, Faisalabad, Pakistan, pp. 225-231.

ASTM D1545-07 (2012). "Standard test method for viscosity of transparent liquids by bubble time method," ASTM International, West Conshohocken, USA.

Béland, M. C., Lindberg, S., and Johansson, P. A. (2000). "Optical measurement and perception of gloss quality of printed matte-coated paper," *J. Pulp Pap. Sci.* 26(3), 120-123.

Biricik, Y., Sonmez, S., and Ozden, O. (2011). "Effects of surface sizing with starch on physical strength properties of paper," *Asian J. Chem.* 23(7), 3151-3154.

Bismarck, A., Baltazar-Y-Jimenez, A., and Sarikakis, K. (2006). "Green composites as panacea? Socio-economic aspects of green materials," *Environment, Development and Sustainability* 8(3), 445-463. DOI: 10.1007/s10668-005-8506-5

DIN 16945 (1989). "Testing of resins, hardeners and accelerators, and catalyzed resins," Beuth Verlag GmbH, Berlin, Germany.

DIN EN ISO 175 (2011). "Plastics - Methods of test for the determination of the effects of immersion in liquid chemicals," Beuth Verlag GmbH, Berlin, German.

DIN EN ISO 178 (2013). "Plastics - Determination of flexural properties," Beuth Verlag GmbH, Berlin, Germany.

DIN EN ISO 527-2 (2012). "Plastics - Determination of tensile properties - Part 2: Test conditions for moulding and extrusion plastics," Beuth Verlag GmbH, Berlin, Germany.

DIN EN ISO 2811-1 (2011). "Paints and varnishes - Determination of density - Part 1: Pyknometer method," Beuth Verlag GmbH, Berlin, Germany.

DIN EN ISO 4288 (1998). "Geometrical Product Specifications (GPS) - Surface texture: Profile method - Rules and procedures for the assessment of surface texture," Beuth Verlag GmbH, Berlin, Germany.

Duratek (2016). "Duratek 1200: Solvent-free epoxy lamination resin," (https://www.duratek.com.tr), Accessed 23 July 2016.

Elmas, G. M., and Sonmez, S. (2011). "Printability properties of some alkaline sulfite-anthraquinone-methanol handsheets," *Asian J. Chem.* 23(6), 2515-2519.

Fairchild, M. D. (2004). "Color appearance models: CIECAM02 and beyond", (http://rit-mcsl.org/fairchild/PDFs/AppearanceLec.pdf), Accessed 25 July 2016.

Genc, G. (2015). "Dynamic properties of *Luffa cylindrica* fiber reinforced bio-composite beam," *Journal of Vibroengineering* 17(4), 1615-1622.

Genc, G., and Koruk, H. (2016a). "On the difficulties in manufacturing of luffa fibers reinforced bio-composites and variations in their dynamic properties," in: *Proceedings of the 45th International Congress and Exposition on Noise Control Engineering INTER-NOISE 2016*, Hamburg, Germany, pp. 1572-1576.

Genc, G., and Koruk, H. (2016b). "Investigation of the vibro-acoustic behaviors of luffa bio composites and assessment of their use for practical applications," in:

Proceedings of the 23rd International Congress on Sound and Vibration (ICSV23), Athens, Greece, pp. 1-8.

Ilhan, M. (2014). "Synthesis, structure and photoluminescence properties of Ho^{3+} doped TTB-$BaTa_2O_6$ phosphors," *Solid State Sci.* 38, 160-168. DOI: 10.1016/j.solidstatesciences.2014.08.015

IPC (2016). "IPC-TM-650 test methods manual: Adhesion, tape testing," (https://www.ipc.org/TM/2.4.1E.pdf), Accessed 03 August 2016.

ISO 2813 (2014). "Paints and varnishes - Determination of gloss value at 20 degrees, 60 degrees and 85 degrees," International Organization for Standardization, Geneva, Switzerland.

Johnson, J., Andersson, C., Lestelius, M., Järnström, L., Rättö, P., and Blohm, E. (2009). "Some properties of flexographic printing plates and aspects of print quality," *Appita J.* 62(5), 371-378.

Juuti, M., Prykäri, T., Alarousu, E., Koivula, H., Myllys, M., Lähteelä, A., Toivakka, M., Timonen, J., Myllylä, R., and Peiponen, K. E. (2007). "Detection of local specular gloss and surface roughness from black prints," *Colloid. Surface. A* 299(1-3), 101-108. DOI: 10.1016/j.colsurfa.2006.11.039

Khalid, M., and Mohammad, F. (2009). "Preparation, FTIR spectroscopic characterization and isothermal stability of differently doped fibrous conducting polymers based on polyaniline and nylon-6,6," *Synthetic Met.* 159 (1-2), 119-122. DOI: 10.1016/j.synthmet.2008.08.005

Koçak, E. D. (2008). "The influence of ultrasonic energy on chemical treatment of surface properties and the properties of composites made of luffa cylindrical fiber-polyester resin," *J. Eng. Mater. Technol.* 130(4), 1-7. DOI: 10.1115/1.2969251

Koruk, H., and Genc, G. (2015). "Investigation of the acoustic properties of bio luffa fiber and composite materials," *Mater. Lett.* 157, 166-168. DOI: 10.1016/j.matlet.2015.05.071

Mohanta, N., and Acharya, S. K. (2013). "Tensile, flexural and interlaminar shear properties of *Luffa cylindrica* fibre reinforced epoxy composites," *International Journal of Macromolecular Science* 3(2), 6-10.

Mohanta, N., and Acharya, S. K. (2015). "Investigation of mechanical properties of *Luffa cylindrica* fibre reinforced epoxy hybrid composite," *International Journal of Engineering, Science and Technology* 7(1), 1-10. DOI: 10.4314/ijest.v7i1.1

Mohanty, A. K., Misra, M., and Hinrichsen, G. (2000). "Biofibres, biodegradable polymers and biocomposites: An overview," *Macromol. Mater. Eng.* 276-277(1), 1-24. DOI: 10.1002/(SICI)1439 2054(20000301)276:1<1: :AID-MAME1>3.0.CO;2-W

Preston, J. S., Elton, N. J., Husband, J. C., Dalton, J., Heard, P. J., and Allen, G. C. (2002). "Investigation into the distribution of ink components on printed coated paper: Part 1: Optical and roughness considerations," *Colloid. Surface. A* 205(3), 183-198. DOI: 10.1016/S0927-7757(02)00020-1

Scudamore, R. J., and Cantwell, W. J. (2002). "The effect of moisture and loading rate on the interfacial fracture properties of sandwich structures," *Polym. Composite.* 23(3), 406-417. DOI: 10.1002/pc.10442

Sonmez, S. (2011). "Interactive effects of copolymers and nano-sized pigments on coated recycled paperboards in flexographic print applications," *Asian J. Chem.* 23(6), 2609-2613.

Tanobe, V. O. A., Flores-Sahagun, T. H. S., Amico, S. C., Muniz, G. I. B., and Satyanarayana, K. G. (2014). "Sponge gourd (*Luffa cylindrica*) reinforced polyester

composites: Preparation and properties," *Defence Sci. J.* 64(3), 273-280. DOI: 10.14429/dsj.64.7327

TAPPI T 558 (2010). "Surface wettability and absorbency of sheeted materials using an automated contact angle tester," TAPPI Press, Atlanta, GA, USA.

Viscarra Rossela, R. A., Minasnya, B., Roudiera, P., and McBratneya A. B. (2006). "Colour space models for soil science," *Geoderma* 133(3-4), 320-337. DOI: 10.1016/j.geoderma.2005.07.017

Wang, L. L., Tay, B. K., See, K. Y., Sun, Z., Tan, L. K., and Lua, D. (2009). "Electromagnetic interference shielding effectiveness of carbon-based materials prepared by screen printing," *Carbon* 47(8), 1905-1910. DOI: 10.1016/j.carbon.2009.03.033

Zang, Y. H., and Aspler, J. S. (1995). "The influence of coating structure on the ink receptivity and print gloss of model clay coatings," *Tappi J.* 78(1), 147-154.

Article submitted: September 7, 2016; Peer review completed: November 20, 2016; Revised version received: November 21, 2016; Accepted: November 22, 2016; Published: December 5, 2016.
DOI: 10.15376/biores.12.1.760-773